SIMULATION OF DUCTILE FRACTURE OF S235JR STEEL USING COMPUTATIONAL CELLS WITH MICROSTRUCTURALLY-BASED LENGTH SCALES

Paweł Grzegorz Kossakowski

Faculty of Civil and Environmental Engineering, Kielce University of Technology, Kielce, Poland
e-mail: kossak@tu.kielce.pl

The paper presents results of a numerical modelling of ductile fracture and failure of elements made of S235JR steel subjected to static tension. The analysis was performed using the Gurson-Tvergaard-Needleman (GTN) model, which takes into consideration the material structure. The GTN material parameters of S235JR steel were assumed basing on the results of its microstructural and strength properties. The aim of the research was to specify and test the procedure that enables one to perform engineering calculations of tensioned structural elements using the GTN material model. During numerical simulations, the mesh size-effect was analysed, basing on microstructurally-based length scales methods. The results show high sensivity of strength curves in the range from the maximum force to the failure depending on the method and mesh size applied.

Key words: Gurson-Tvergaard-Needleman model, voids, numerical calculations, S235JR steel

1. Introduction

The analysis of plastic ranges is a fundamental issue undertaken in both research as well as in ordinary engineering practice. From practical point of view, it is particularly important to estimate the limit loads beyond the elastic range for structural elements, especially when operating in the pre-failure condition.

The failure of a material is dependent on more than one major stress, and the safety of a steel structure can be assessed using the so called Huber-Mises-Hencky (HMH) strength hypotheses. A number of studies show that the HMH model is not always suitable to analyse the plastic state in and beyond the

range of deformations corresponding to the necking of an element subjected to tension. Assuming the continuum of the material, one cannot apply this model to establish the influence of microstructural defects on the material strength.

The processes of crack initiation and propagation in polycrystalline structures are closely related to the material microstructure. There are several basic types of fracture mechanisms, i.e. plastic, cleavage and brittle intergranular, shear or void-sheeting and ductile (Teirlinck *et al.*, 1988). In shear and ductile fracture, the cracking is attributable to the nucleation, growth and coalescence of voids (Fig. 1).
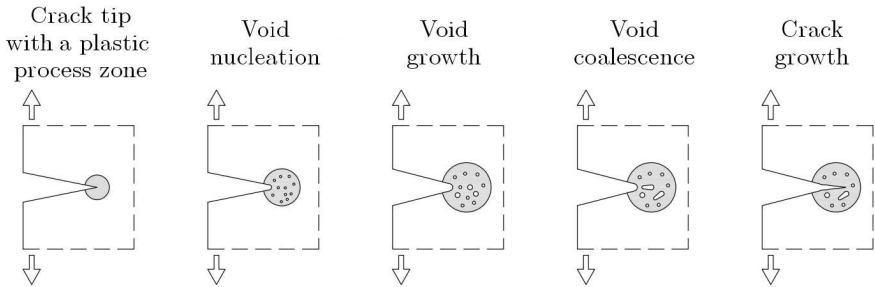

Fig. 1. Scheme of void evolution (basing on Sedlacek *et al.* (2008))

Damage in form of voids occurs on the existing inclusions and second-phase particles. The growth and coalescence of these voids (Fig. 2) result in the development of localised plastic deformations.
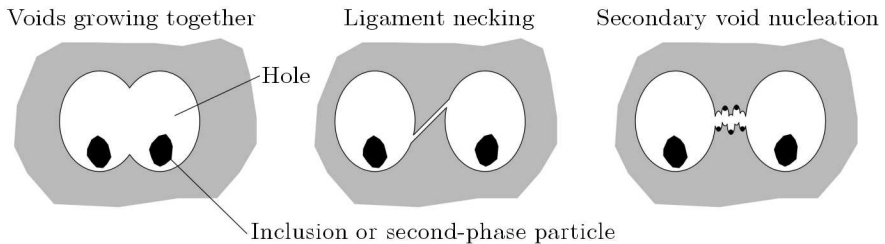

Fig. 2. Types of void coalescence (basing on Sedlacek *et al.* (2008))

The phenomenon described above can be analysed using damage models taking into account the influence of microstructural defects on the material strength by defining a relationship between the particular failure stages and the strength of the material. The Gurson (1977) model for a porous solid is one of such models. It is a modified Huber-Mises-Hencky criterion, defining the influence of an increase in the void volume fraction on the strength of the material. This model was further modified by Tvergaard (1981) and then

by Tvergaard and Needleman (1984), and Needleman and Tvergaard (1984), who developed a method for the calculation of failure loads resulting from ductile fracture by considering selected microstructural parameters and plastic properties of a material. The Gurson-Tvergaard-Needleman model is referred to as the GTN model.

It should be emphasised that the GTN model is a basic damage model recommended to use in the analysis of emergency condition for building structures according to the current standards, for instance PN-EN 1993-1-10 (2007) and its commentary by Sedlacek *et al.* (2008).

A number of studies carried out by authors (also by Kossakowski, 2009, 2010; Kossakowski and Trąmpczyński, 2011) show that, for alloys and structural steels, the GTN model ensures a better consistency of the strength curves obtained by numerical calculation (modelling) with experimental results than the HMH criterion. Most results are obtained by the authors by conducting simple strength tests, mainly tensile strength tests. Numerical analyses are performed using the method of best fit to material constants (the GTN model) for elements with predetermined geometries and strength properties. The GTN model parameters are frequently determined basing on the fitting curve technique. Another drawback is the lack of standardised microstructural parameters to develop a GTN model for steels used most commonly in civil engineering.

Numerical strength analysis of structural elements in the nonlinear range is another problem. When simulating ductile fracture using the finite element method, in particular, using the GTN model, size effects are encountered. It reveals the softening of the final part of the strength curve. Several methods have been tested (eg. Tvergaard and Needleman, 1995; Ramaswamy and Avaras, 1998; Borino *et al.*, 2003) to minimize the softening effect, but many of them cannot be applied due to limitations in available engineering software.

All these problems require development of a procedure for numerical modelling of the load limit for structural elements, taking into account the effect of microfailure. From practical point of view, it is particularly important to specify the procedures to carry out engineering calculations using the GTN material model.

Therefore, the aim of the research was to specify and test the procedure that enables one to perform engineering calculations of tensioned structural elements using the GTN material model. This paper includes results of a numerical modelling of elements made of S235JR steel subjected to static tension, basing on the Gurson-Tvergaard-Needleman (GTN) model, taking into consideration the real material structure. S235JR steel was selected for

the tests because it is a common structural material in Poland as well as in other European countries.

For S235JR steel, the elastic-plastic material model was elaborated through testing of various approximation stress-strain curves. The GTN material parameters were assumed basing on the results of microstructural and strength properties of S235JR steel and the results of analysis performed before by Kossakowski (2009, 2010), and Kossakowski and Trąmpczyński (2011).

During numerical simulations, the mesh size-effect was analysed, basing on the microstructurally-based length scales methods.

It should be noticed that the presented data may be used for any analyses and expertise connected with the assessment of the load-carrying capacity and safety of structural elements, especially made of S235JR steel.

2.   Gurson-Tvergaard-Needleman (GTN) damage model

The first model to take into consideration microdamage (pores, voids) was the Gurson (1977) model, which assumed that the proportion of voids in the plastic potential function was dependent on the void volume fraction f. The original Gurson condition was modified by Tvergaard (1981) and Tvergaard and Needleman (1984) as

$$\Phi = \left(\frac{\sigma_e}{\sigma_0}\right)^2 + 2q_1 f^* \cosh\left(-q_2\frac{3\sigma_m}{2\sigma_0}\right) - (1 + q_3 f^{*2}) = 0 \qquad (2.1)$$

where: σ_e – von Mises effective stress according to the HMH hypothesis, σ_0 – yield stress of the material, σ_m – hydrostatic pressure (mean stress), f^* – actual void volume fraction, q_i – Tvergaard coefficients describing the plastic properties of the material.

In the GTN model, the void volume fraction f^* is defined as follows

$$f^* = \begin{cases} f & \text{for} \quad f \leqslant f_c \\ f_c + \dfrac{\overline{f}_F - f_c}{f_F - f_c}(f - f_c) & \text{for} \quad f_c < f < f_F \\ \overline{f}_F & \text{for} \quad f \geqslant f_F \end{cases} \qquad (2.2)$$

where: f_c – critical void volume fraction at which the void coalescence starts, f_F – void volume fraction corresponding to the complete loss of the material strength, at the final separation of the material, and $\overline{f}_F = (q_1 + \sqrt{q_1^2 - q_3})/q_3$.

An increase in the void volume fraction $\dot{f}$ is defined by the relationship

$$\dot{f} = \dot{f}_{gr} + \dot{f}_{nucl} = (1 - f)\dot{\varepsilon}^{pl} : \mathsf{I} + \frac{f_N}{s_N\sqrt{2\pi}} \exp\left[-\frac{1}{2}\left(\frac{\varepsilon_{em}^{pl} - \varepsilon_N}{s_N}\right)^2\right]\dot{\varepsilon}_{em}^{pl} \quad (2.3)$$

where: $\dot{f}_{gr}$ – change due to growth of voids existing in the material, $\dot{f}_{nucl}$ – change due to nucleation of new voids, f_N – volume fraction of nucleated voids, s_N – standard deviation of nucleation strain, $\dot{\varepsilon}^{pl}$ – plastic strain rate tensor, I – second-order unit tensor, ε_N – mean strain of the void nucleation, ε_{em}^{pl} – equivalent plastic strain in the matrix material, $\dot{\varepsilon}_{em}^{pl}$ – equivalent plastic strain rate in the matrix material.

3. Microstructurally-based length scales methods used in simulations of ductile fracture

As mentioned before, during numerical simulations with using the finite element method, the mesh-size effect can be encountered. For analysis of nonlinear ranges, especially when a GTN model is used, this effect reveals the softening of the final part of the strength curve. In order to take into account and examine this phenomenon, two microstructurally-based length scales methods were used in the presented study.

3.1. SMCS-based method

Different models were applied to describe the initiation of ductile fracture which is affected by many processes, such as initial distribution of voids, anisotropy and evolution of spacing and shape of the built-in inclusions, void nucleation, void-to-void interactions and the nucleation and growth of secondary voids near coalescence. Assuming the void growth to be the most significant element during the ductile fracture process, the void nucleation strains can be ignored. The void coalescence is considered through a critical void ratio, and void-to-void interactions and localization in the intervoid ligaments are neglected. According to McClintock (1968) and Rice and Tracey (1969), the void growth is dependent on the evolution of two main quantities, the equivalent plastic strain ε_e^{pl}, and the stress triaxiality σ_m/σ_e. One of the models based on given assumptions is the Stress Modified Critical Strain (SMCS) model, proposed by Hancock and Mackenzie (1976) and Panontin and Sheppard (1995).

According to the SMCS criterion, in order to form a crack, the limiting critical value on stresses and plastic strain must be exceeded over the critical volume of material.

In two dimensions, the critical volume is defined by a characteristic length measure l_c in the region of high stresses and plastic strain, as shown in Fig. 3. The contours represent the difference between the equivalent plastic strain ε_e^{pl} and the critical equivalent plastic strain $\varepsilon_{e\,critical}^{pl}$ at each loading step ahead of a crack tip.
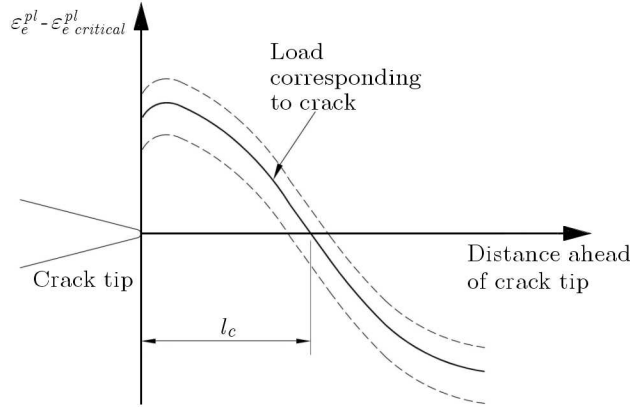

Fig. 3. Predicting ductile crack initiation defined by the characteristic length l_c (basing on Kanvinde and Deierlein (2006))

The SMCS fracture initiation criteria can be written as

$$\varepsilon^{pl} > \varepsilon_{critical}^{pl} \qquad \text{over} \qquad r > l_c \tag{3.1}$$

The fracture criterion is satisfied over a progressively increasing distance until it is satisfied over the characteristic length, and formation of a crack is predicted. The solid contour corresponds to the first loading step when the criterion is satisfied over the characteristic length l_c, corresponding to fracture initiation.

To ensure the opportunity to initiate ductile fracture during numerical simulation, it is necessary to apply a proper mesh size. It is especially important in the region with high stress-strain gradients, for instance near the crack tip. The SMCS fracture criterion can be satisfied for cell dimensions, identified with the mesh size, exceeded over the critical volume of material, represented by the characteristic length l_c. Thus, the mesh dimension D should be equal to the characteristic length l_c at least.

3.2. Cell model-based method

As mentioned at the beginning, many metals fail due to growth of the void. This mechanism displays a macroscopically planar fracture process zone of one or two void spacings in thickness. It is characterised by intense plastic flow in the ligaments between the voids. Outside the fracture process zone, the voids exhibit little or no growth (Xia and Shih, 1995a,b; Gao *et al.*, 1998; Faleskog *et al.*, 1998; Kossakowski and Trąmpczyński, 2011).

In order to model the process described above, a layer of the material containing a pre-existing population of similar sized voids is assumed. A single row of computational cells of the linear dimension D represents this layer. Each computational cell contains a single void of some initial volume f_0. The thickness of this layer D is interpreted as the mean spacing between the voids nucleated from large inclusions. Microvoids nucleated from small inclusions assist the process of hole link-up with the crack tip and can be taken into account in the coalescence phase. Cells near the newly formed crack surface have undergone significant void growth, while cells further away exhibit little or no void growth. The void growth is described by the Gurson constitutive relation for dilatant plasticity, resulting in material softening and, ultimately, loss of stress carrying capacity. The material outside this strip is undamaged by void growth and described by elastic-plastic relation (Fig. 4).
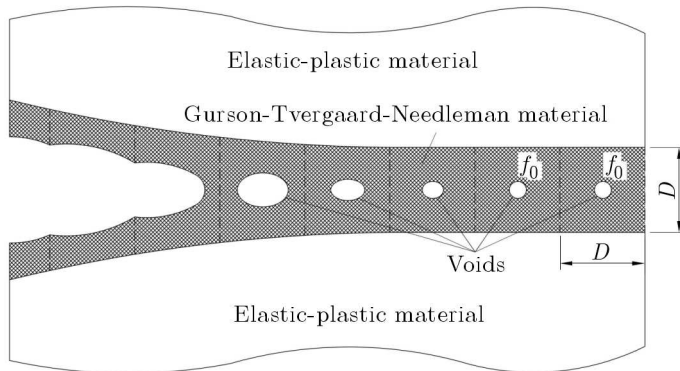

Fig. 4. The region near the crack tip modelled according to the Cell model method (basing on Gao *et al.* (1998), Faleskog *et al.*, 1998))

4. Microstructurally-based length scales examinations for S235JR steel

The first step of the material analysis was to obtain microstructural images of S235JR steel with a ferritic-perlitic matrix with a large number of non-metallic

inclusions. S235JR steel was reported to have appropriate metallurgical purity. To fully characterize the non-metallic inclusions in the material, it was necessary to determine the basic stereological parameters. The void volume fraction was $f_0 = 0.0017 = 0.17\%$ (Kossakowski, 2010).

As described before, to form a macroscopic crack, the fracture criterion must be satisfied over the minimum volume of the material defined in two dimensions by the characteristic length measure l_c in the region of high stresses and plastic strain. Several approaches have been discussed, but determination of the length scale is subjective (e.g. Panontin and Sheppard, 1995; Chi *et al.*, 2006; Rousselier, 1987). In the presented study, an approach based on that proposed by Hancock and Mackenzie (1976) was used. According to the assumption of this method, the linking of two or more holes formed from coalescing inclusion colonies leads to fracture. Thus a macrocrack formation only occurs when shear localizes between multiple clusters, while void growth expands the cluster of inclusion colonies. The size of these inclusion colonies represents the length scale and is visible in a fractograph. In the presented study, the characteristic length l_c was determined as the dimension of plateau and valley on the fracture surface (Fig. 5). The measurement was performed for twenty inclusion colonies using the statistical Chauvenet criterion. All atypical values were rejected. The characteristic length l_c ranged from $130\,\mu$m to $360\,\mu$m, with the mean value of l_c being $\approx 250\,\mu$m.
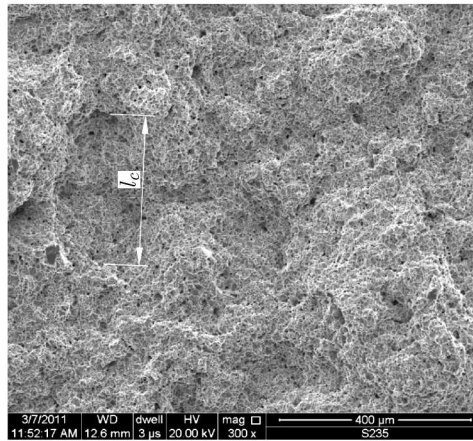

Fig. 5. Determining the characteristic length l_c defined by dimensions of plateaus and valleys

While the characteristic length l_c was based on dimensions of plateaus and valleys, the length D was defined as the mean spacing between the voids nucleated from large inclusions and determined during the microstructural

examinations as well. As mentioned above, a large number of non-metallic inclusions, which were mainly sulphides and brittle oxides, were noticed in the microstructure of S235JR steel.

Sulfide inclusions were elongated in shape, and their distribution in the volume was irregular. They were arranged in bands. Other non-metallic inclusions found in the tested materials are uniaxial brittle oxide inclusions, which may co-occur with sulfide inclusions. In order to determine the length D, a statistical procedure was used similarly as for the characteristic length l_c. The length of D ranged from $40\,\mu$m to $180\,\mu$m, with the mean value of D being $\approx 100\,\mu$m (Fig. 6).
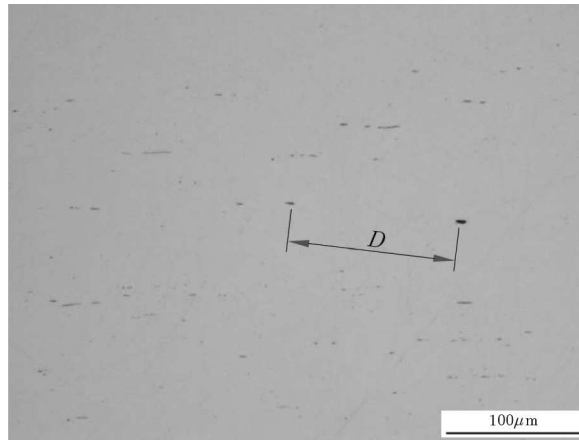

Fig. 6. Determining the length D defined by mean spacing between the voids nucleated from large inclusions

5. Determination of GTN model parameters

The first step was to perform static tensile strength tests for specimens with a circular cross-section, according to PN-EN10002-1 (2004). The nominal diameter of the specimens was $\phi = 10\,$mm, the length of the measuring base $l_0 = 50\,$mm, and the primary cross-sectional area $S_0 = 78.5\,$mm^2. The average values obtained during the tests were as follows: the yield stress $R_{0.2} = 318\,$MPa, the tensile strength $R_m = 446\,$MPa, and the displacement percentage $A_5 = 33.9\%$. Using the averaged $\sigma(\varepsilon)$ curve, it was possible to determine the nominal normal stress σ and the longitudinal strain ε.

The parameters of the GTN model for S235JR steel were established on the basis of microstructure analysis, numerical modelling of tensile strength tests,

and results of the analysis performed before by Kossakowski (2009, 2010), and Kossakowski and Trąmpczyński (2011).

The initial void volume fraction was determined during the microstructure analysis as $f_0 = 0.0017 = 0.17\%$. The Tvergaard parameters were determined according to the results obtained by Faleskog *et al.* (1998). For the ratio $R_{0.2}/E = 0.00155$ and strain-hardening exponent $N = 0.195$, the values of Tvergaard parameters were established as $q_1 = 1.91$, $q_2 = 0.79$ and $q_3 = 3.65$. The other parameters of the GTN model were defined numerically, basing on the studies by Kossakowski (2009, 2010), and Kossakowski and Trąmpczyński (2011). The numerical calculations were performed using a program based on the finite element method, Abaqus Explicit version 6.10. The elements were modelled as axially symmetrical components using standard elements (Abaqus, 2010).

The averaged tensile strength curve was approximated by the equation

$$
\varepsilon = \begin{cases}
\dfrac{\sigma}{E} & \text{for} \quad \sigma < \sigma_0 \\[2ex]
\dfrac{\varepsilon_1 - \varepsilon_0}{\sigma_1 - \sigma_0}(\sigma - \sigma_0) + \varepsilon_0 & \text{for} \quad \sigma_0 \leqslant \sigma \leqslant \sigma_1 \\[2ex]
\varepsilon_0 + \dfrac{\sigma_{01}}{E}\Big(\dfrac{\sigma}{\sigma_{01}}\Big)^{1/N} & \text{for} \quad \sigma > \sigma_1
\end{cases}
\tag{5.1}
$$

where: ε – strain, ε_0 – yield strain, ε_1 – initial hardening strain, σ – stress, σ_0 – yield stress, σ_1 – initial hardening stress, σ_{01} – initial stress at the beginning of the nonlinear part of the approximation curve, E – modulus of elasticity, N – strain-hardening exponent.

The parameters of the GTN model were determined basing on the $\sigma(\varepsilon)$ curves obtained through numerical analysis and experiments. At each iteration step, the values of the GTN model parameters were changed within certain limits. The optimization criterion was the convergence of the $\sigma(\varepsilon)$ values obtained numerically and experimentally.

The critical void volume fraction, f_c, above which the nominal material strength decreased, was determined as 0.06, basing on the determined value of f_0, as suggested by Richelsen and Tvergaard (1994). The value of the void volume fraction corresponding to the complete loss of material strength f_F was assumed as 0.667. The volume fraction of the nucleated voids f_N was 0.04, the average nucleation strain of inclusion-related voids ε_N was 0.3, and the standard deviation of the strain s_N was 0.05. All parameters of the GTN model are summarized in Table 1.
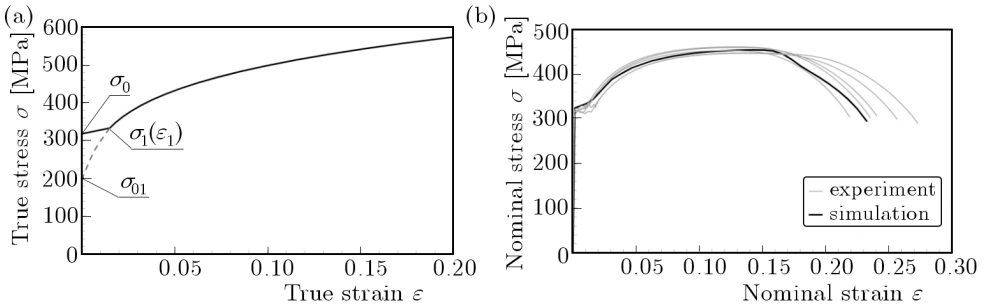
Fig. 7. The approximation of the true stress-strain $\sigma(\varepsilon)$ curve (a) and nominal stress-strain $\sigma(\varepsilon)$ curves (b) of S235JR steel

Table 1. Microstructural parameters of the GTN model of S235JR steel

f_0	f_c	f_F	q_1	q_2	q_3	ε_N	f_N	s_N
0.0017	0.06	0.667	1.91	0.79	3.65	0.3	0.04	0.05

6. Numerical simulation of ductile fracture of S235JR steel using computational cells with microstructurally-based length scales

The numerical analysis was also performed using Abaqus Explicit version 6.10. The elements modelled were the same as those used during the tensile strength tests. The specimens with a circular cross-section were subjected to quasi-static tension and a displacement control increase with the strain rate $\dot{\varepsilon} = 0.1\,\mathrm{s}^{-1}$. The modelling was performed for axially symmetrical elements. Because of the symmetry, the modelling was conducted only for half-specimens (Fig. 8). A sharp notch with a depth of $R = 0.05\,\mathrm{mm}$ was modelled in the middle of the sample length. During numerical simulations, two approaches based on computational cells with microstructurally-based length scales were applied.

Two models were used during the numerical simulations. For the first one, referred as *GTN model*, the damaged Gurson-Tvergaard-Needleman material model was assumed for the whole numerical model. The dimensions of the cell localised near the crack plane were equal to $D \times D/2$, where D was equal to the characteristic length $l_c = 250\,\mu\mathrm{m}$ determined during microstructural examinations.

The second model, referred as *Cell model*, was based on the assumptions given in the previous section. The elements adjacent to the crack plane were modelled by making use of the GTN material model. Their dimensions were equal to $D \times D/2$. The value of D was equal to the mean spacing between the
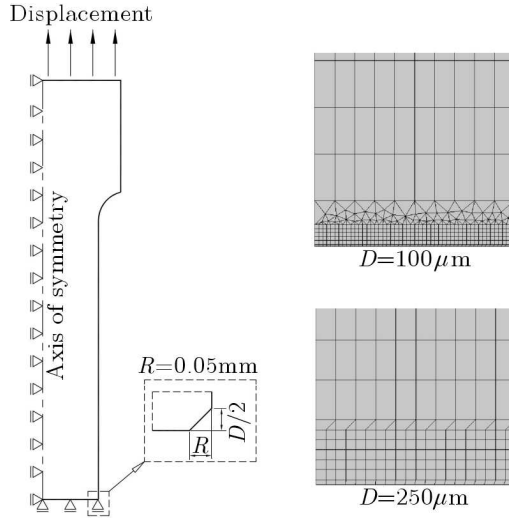
Fig. 8. Geometry of numerical models used during simulations

large voids $D = 100\,\mu$m. The simulations were also conducted for cell dimensions $D = 250\,\mu$m, based on the characteristic length l_c. The elastic-plastic material model was assumed for the rest of the numerical model according to Fig. 4.

The numerical simulations of ductile fracture of S235JR steel were based on the force-elongation $F(l)$ curves. The analysis began with the determination of the coefficients of approximation equation (5.1). The yield stress was established according to the values obtained during the tests, i.e. $\sigma_0 = 318$ MPa. It was found that the strain-hardening exponent N had a very significant impact on the force F and elongation l determined numerically. The optimization condition was the convergence of the force-elongation $F(l)$ values obtained numerically and experimentally using the mean square error criterion. For all analysed cases, the best agreement of the results was achieved for the strain-hardening exponent $N = 0.195$. Force-elongation curves $F(l)$ determined during experiments and simulations by using *GTN* and *Cell models* are shown in Figs. 9-11. For comparison, the curves determined assuming $N = 0.19$ and $N = 0.20$ are also shown. Others constants of approximation equation (5.1) were determined as follows: yield strain $\varepsilon_0 = 0.002$, initial hardening strain $\varepsilon_1 = 0.015$, initial hardening stress $\sigma_1 = 333$ MPa, initial stress at the beginning of the nonlinear part of the approximation curve $\sigma_{01} = 198$ MPa, and modulus of elasticity $E = 205$ GPa.

It should be noted that the tensile strength curves obtained by applying *GTN model* were consistent with the experimental results in the first range, until the maximum force F was reached.

In the range from the maximum force to failure, the forces F determined during the experiments were higher than those found from numerical simulations using *GTN model*. There was a sharp decrease in the force corresponding to elongation equal to ~ 8.0 mm, followed by the element failure after the maximum force was reached (Fig. 9). The visible softening was noticed when *GTN model* was used for the whole numerical model. The simulated failure of elements was noticed for elongation equal to 11.7-12.0 mm, depending on the strain-hardening exponent N.
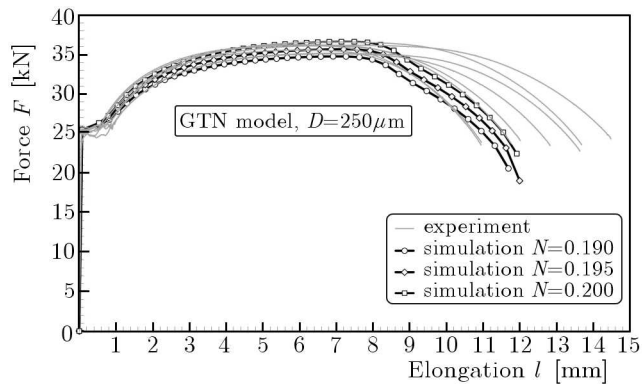

Fig. 9. Force-elongation $F(l)$ curves determined during experiments and numerical simulations by using *GTN model* with $D = 250\,\mu$m
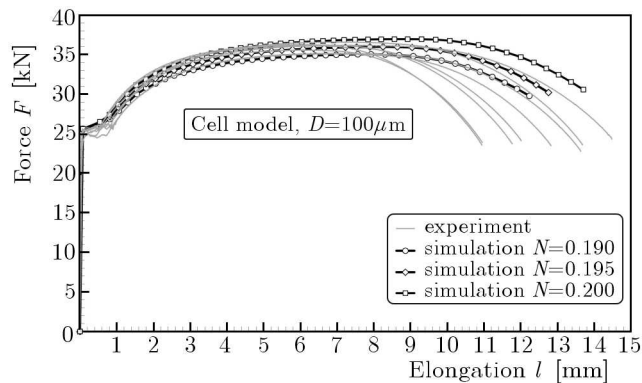

Fig. 10. Force-elongation $F(l)$ curves determined during experiments and numerical simulations by using *Cell model* with $D = 100\,\mu$m

Good agreement of the results in the first range of strength curves was also found when *Cell model* was used. For cell dimensions $D = 100\,\mu$m, the forces F established by numerical simulations were higher than those determined in experiments in the final part of force-elongation $F(l)$ curves (Fig. 10).
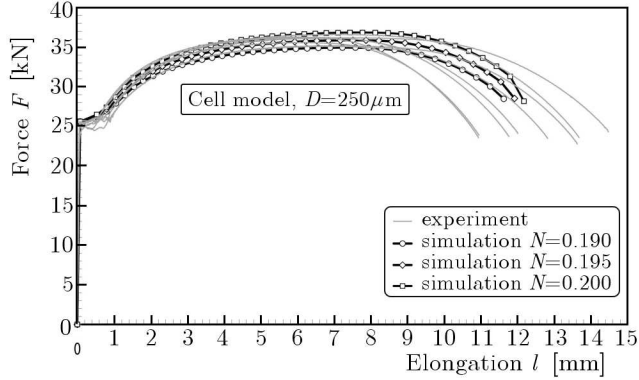

Fig. 11. Force-elongation $F(l)$ curves determined during experiments and numerical simulations by using *Cell model* with $D = 250\,\mu$m

In the whole range of strength curves the best agreement of results was noticed for dimension $D = 250\,\mu$m (Fig. 11). The simulated failure of elements was noticed for elongation equal to 12.3-13.7 mm and 11.7-12.2 mm, depending on the strain-hardening exponent N for dimension $D = 100\,\mu$m and $D = 250\,\mu$m, respectively.

7.   Discussion

As shown in the previous section, it was possible to numerically simulate ductile fracture and failure of elements made of S235JR steel subjected to static tension taking into consideration effects of microstructural defects. It should be noted that the tensile strength curves obtained by applying both *GTN* and *Cell model* were more or less consistent with the experimental results.

In all cases, the best agreement was achieved by assuming a strain-hardening exponent $N = 0.195$. In the first range until the maximum force was reached, the strength curves obtained by applying both *GTN* and *Cell models* were fully consistent with the experimental results. However, in the further part of the tensile strength curves, differences were noticed depending on the model assumed. The final parts of simulated curves, in the range from the maximum force to failure, were much consistent with the experimental data using

Cell model in comparison to *GTN model*. It is clearly visible in Fig. 12, where experimental and simulated strength curves for the strain-hardening exponent $N = 0.195$ are presented. The softening effect was noticed for elements modelled using *GTN model*, due to significant reduction of the strength through the assuming the voided material for the entire numerical model. A different situation was observed when *Cell model* was used. The values of forces in the final part of tensile curves were much consistent with the experimental data comparing to *GTN model*. During simulations performed using *Cell model*, there was no softening effect.
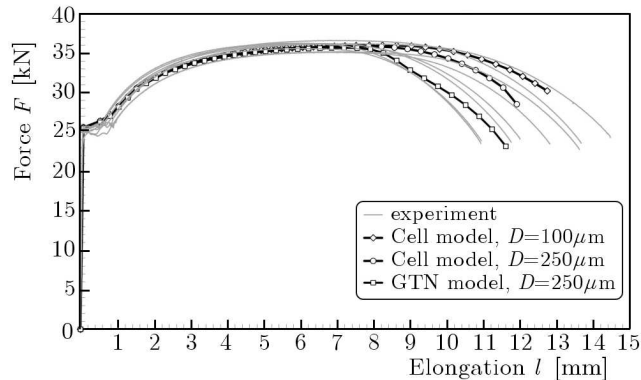

Fig. 12. Force-elongation $F(l)$ curves determined during experiments and numerical simulations by using *GTN* and *Cell models* ($N = 0.195$)

When using *Cell model*, the process zone at the fracture surface is modelled as a layer of the material containing a pre-existing population of similar sized voids, containing a single void of some initial volume f_0. It is close to real situation, because for S235JR steel the fracture mechanism displays a macroscopically planar fracture process zone of one or two void spacings in thickness (Kossakowski and Trąmpczyński, 2011). Outside the fracture process zone, the voids exhibit little or no growth. Considering the above, it can be concluded that applying *Cell model* provides simulation of the ductile failure process close to a real situation in relation to the microstructure of S235JR steel.

As can be seen in Fig. 12, the cell dimension D has impact on results of simulation, revealing in the final part of the force-elongation curves. For the dimension $D = 250\,\mu\text{m}$, values of the force were close to mean experimental data. When using the mesh based on the cell dimension $D = 100\,\mu\text{m}$, the results obtained were higher due to a very small process zone containing voids leading to a smooth reduction of the material strength. It can be concluded

that the modelling of ductile fracture of S235JR using *Cell model* should be performed based on the cell dimension $D = 250\,\mu$m rather than $D = 100\,\mu$m.

When using *Cell model*, it should be noticed that the process zone needs to be assumed *a priori* in the region of potential failure. Unfortunately, for structural elements with complicated geometry, it may be difficult to predict precisely. The process zone determined incorrectly can lead to false results. Therefore, it seems that practical application of *Cell model* method may be limited.

8. Conclusions

The following conclusions have been drawn basing on the results of numerical simulations of ductile fracture of S235JR steel using computational cells with microstructurally-based length scales:

- The numerical analysis showed that by applying the Gurson-Tvergaard-Needleman model, which takes into account the real microstructural parameters for S235JR, it is possible to simulate failure of elements subjected to static tension resulting from ductile fracture.

- In order to simulate ductile fracture of S235JR steel, the averaged tensile strength curve approximated by equation (5.1) is proposed. The best agreement of numerical and experimental results was noticed for the strain-hardening exponent $N = 0.195$ and yield stress obtained during strength tests, i.e. $\sigma_0 = 318\,$MPa.

- The tensile strength curves obtained by applying *GTN model* were consistent with the experimental results in the first range, until the maximum force was reached. However, in the range from the maximum force to failure, the forces F determined during the experiments were higher than those calculated during numerical simulations. Applying *GTN model* for whole numerical models, leads to softening followed by a much more reduction of the material strength in comparison to void growth noticed during the experiments.

- When using *Cell model*, the process zone is modelled as a layer of the material containing a pre-existing population of similar sized voids, containing a single void of some initial volume f_0. It is close to a real situation, because for S235JR steel the fracture mechanism displays a macroscopically planar fracture process zone of one or two void spacings in thickness, while outside the fracture process zone, the voids exhibit little or no growth. The force-elongation curves obtained during numerical simulations were more or less consistent with the experimental data

in the whole range, from the beginning up to failure. Considering the above, it can be concluded that applying *Cell model* provides simulation of the ductile failure process close to a real situation in relation to the microstructure of S235JR steel.

- The results of simulations were much more consistent with strength tests when using *Cell models* with cell dimensions $D = 250\,\mu$m rather than $D = 100\,\mu$m. It was followed by a very small process zone when used cell dimensions $D = 100\,\mu$m interpreted as the mean spacing between the voids nucleated from large inclusions, leading to a smooth reduction of the material strength. When using cell dimensions $D = 250\,\mu$m interpreted as the characteristic length l_c defined by the dimensions of plateaus and valleys formed from coalescing inclusion colonies leading to fracture, the results of simulations were much more consistent with the experimental data.

- Application of *Cell model* requires determination and modelling of the process zone *a priori*. In many cases, it may be difficult to predict it precisely, but the process zone determined incorrectly can lead to false results. Taking the above into consideration, it seems that practical application of *Cell model* method is limited.

References

1. ABAQUS 6.10 Analysis User's Manual, Dassault Systèmes, 2010

2. Borino G., Failla B., Parrinello F., 2003, A symmetric nonlocal damage theory, *International Journal of Solids and Structures*, **40**, 13/14, 3621-3645

3. Chi W.-M., Kanvinde A.M., Deierlein G.G., 2006, Prediction of ductile fracture in steel connections using SMCS criterion, *Journal of Structural Engineering, ASCE*, **132**, 2, 171-181

4. Gao X., Faleskog J., Shih C.F., 1998, Cell model for nonlinear fracture analysis – II. Fracture-process calibration and verification, *International Journal of Fracture*, **89**, 4, 375-398

5. Gurson A.L., 1977, Continuum theory of ductile rupture by void nucleation and growth: Part I – Yield criteria and flow rules for porous ductile media, *Journal of Engineering Materials and Technology, Transactions of the ASME*, **99**, 1, 2-15

6. Faleskog J., Gao X., Shih C.F., 1998, Cell model for nonlinear fracture analysis – I. Micromechanics calibration, *International Journal of Fracture*, **89**, 4, 355-373

7. HANCOCK J.W., MACKENZIE A.C., 1976, On the mechanisms of ductile failure in high-strength steels subjected to multi-axial stress-states, *Journal of Mechanics and Physics of Solids*, **24**, 2/3, 147-160

8. KANVINDE A.M., DEIERLEIN G.G., 2006, The void growth model and stress modified critical strain model to predict ductile fracture in structural steels, *Journal of Structural Engineering*, **132**, 12, 1907-1918

9. KOSSAKOWSKI P., 2009, Analiza nośności oraz rozwoju uszkodzeń stali St3S (S235JRG2) w złożonych stanach naprężenia, *Materiały konferencyjne 55. Konferencji Naukowej KILiW PAN i KN PZITB*, Krynica, 157-164

10. KOSSAKOWSKI P.G., 2010, An analysis of the load-carrying capacity of elements subjected to complex stress states with a focus on the microstructural failure, *Archives of Civil and Mechanical Engineering*, **10**, 2, 15-39

11. KOSSAKOWSKI P.G., TRĄMPCZYŃSKI W., 2011, Numeryczna symulacja zniszczenia stali S235JR z uwzględnieniem wpływu uszkodzeń mikrostrukturalnych, *Przegląd Mechaniczny*, **4**, 15-22

12. MCCLINTOCK F.A., 1968, A criterion for ductile fracture by the growth of holes, *Journal of Applied Mechanics, Transactions ASME Series E*, **35**, 363-371

13. NEEDLEMAN A., TVERGAARD V., 1984, An analysis of the ductile rupture in notched bars, *Journal of the Mechanics and Physics of Solids*, **32**, 6, 461-490

14. PANONTIN T.L., SHEPPARD S.D., 1995, The relationship between constraint and ductile fracture initiation as defined by micromechanical analyses, *Fracture Mechanics: 26th Volume*, ASTM STP 1256, 54-85

15. PN-EN 10002-1:2004 Metallic Materials – Tensile Testing – Part 1: Method of Test at Ambient Temperature

16. PN-EN 1993-1-10:2007 Eurocode 3 – Design of Steel Structures – Part 1-10: Material Toughness and Through-thickness Properties

17. RAMASWAMY S., ARAVAS N., 1998, Finite element implementation of gradient plasticity models. Part II: Gradient dependent evolutions equations, *Computer Methods in Applied Mechanics and Engineering*, **163**, 1/4, 33-53

18. RICE J.R., TRACEY D.M., 1969, On the ductile enlargement of voids in triaxial stress fields, *Journal of the Mechanics and Physics of Solids*, **17**, 3, 201-217

19. RICHELSEN A.B, TVERGAARD V., 1994, Dilatant plasticity or upper bound estimates for porous ductile solids, *Acta Metallurgica et Materialia*, **42**, 8, 2561-2577

20. ROUSSELIER G., 1987, Ductile fracture models and their potential in local approach of fracture, *Nuclear Engineering and Design*, **105**, 1, 97-111

21. Sedlacek G., Feldmann M., Kühn B., Tschickardt D., Höhler S., Müller C., Hensen W., Stranghöner N., Dahl W., Langenberg P., Münstermann S., Brozetti J., Raoul J., Pope R., Bijlaard F., 2008, Commentary and worked examples to EN 1993-1-10 "Material toughness and through thickness properties" and other toughness oriented rules in EN 1993, *JRC Scientific and Technical Reports*, European Commission Joint Research Centre

22. Teirlinck D., Zok F., Embury J.D., Ashby M.F., 1988, Fracture mechanism maps in stress space, *Acta Metallurgica*, **36**, 5, 1213-1228

23. Tvergaard V., 1981, Influence of voids on shear band instabilities under plane strain conditions, *International Journal of Fracture*, **17**, 4, 389-407

24. Tvergaard V., Needleman A., 1984, Analysis of the cup-cone fracture in a round tensile bar, *Acta Metallurgica*, **32**, 1, 157-169

25. Tvergaard V., Needleman A., 1995, Effects of nonlocal damage in porous plastic solids, *International Journal of Solids and Structures*, **32**, 8/9, 1063-1077

26. Xia L., Shih C.F., 1995a, Ductile crack growth – I. A numerical study using computational cells with microstructurally-based length scales, *Journal of the Mechanics and Physics of Solids*, **43**, 2, 233-259

27. Xia L., Shih C.F., 1995b, Ductile crack growth – II. Void nucleation and geometry effects on macroscopic fracture behavior, *Journal of the Mechanics and Physics of Solids*, **43**, 12, 1953-1981

Symulacja pękania ciągliwego stali S235JR z zastosowaniem elementów zdefiniowanych na podstawie mikrostrukturalnych skal długości

Streszczenie

W artykule przedstawiono wyniki modelowania numerycznego pękania ciągliwego oraz zniszczenia elementów wykonanych ze stali S235JR poddanych statycznemu rozciąganiu. W analizie oparto się na modelu materiałowym Gursona-Tvergaarda-Needlemana (GTN), uwzględniającym strukturę materiałową. Parametry materiałowe modelu GTN stali S235JR przyjęto w oparciu o jej własności mikrostrukturalne i wytrzymałościowe. Celem badań było opracowanie i weryfikacja procedury umożliwiającej przeprowadzanie obliczeń inżynierskich rozciąganych elementów konstrukcyjnych przy zastosowaniu modelu GTN. Podczas symulacji numerycznych uwzględniono efekt wielkości siatki, stosując metody oparte na mikrostrukturalnych skalach długości. Uzyskane wyniki ujawniają wysoką wrażliwość krzywych wytrzymałościowych w zakresie od obciążenia maksymalnego do zniszczenia, w zależności od metody oraz wielkości siatki zastosowanej w obliczeniach.